

# End-to-end trajectory design of a mission to the Jovian Trojan asteroids

Tiago J. A. S. Bento  
tiagojasbento@tecnico.ulisboa.pt

Instituto Superior Técnico, Lisboa, Portugal

September 2016

## Abstract

Inspired by the diversity and scientific interest of the Jovian Trojan asteroids, this work deals with the trajectory design of a mission to this system. Two different types of missions are considered: a rendezvous with asteroid 624 Hektor, and a flyby tour of different objects. For both of them, MGA and MGA-1DSM models are utilized to optimize the interplanetary trajectories to the Trojan system. These were adapted from GTOP's code [11], in order to increase their theoretical accuracy and assure quality of results. Additionally, an optimization algorithm survey and tuning study are presented for the MGA implementation, as to fill the gaps found in the literature. For the asteroid flyby tour, a new optimization problem is developed and implemented in this report. This allows for a more efficient optimization of the total flyby tour trajectory. The designed trajectory to 624 Hektor followed a MGA path of Earth-Mars-Jupiter, resulting in a total on-board  $\Delta V$  of 2.4672 km/s. As for the asteroid flyby tour, the MGA route consisted of a Earth-Venus-Mercury-Venus trajectory, leading to the observation of 6 total asteroids. The on-board  $\Delta V$  for this result was 2.3903 km/s, showing improvements over the designs found in Canalias et al. [7].

**Keywords:** Trajectory optimization, Jovian Trojan asteroids, Asteroid flyby tour, Asteroid rendezvous, Multiple gravity assists

## 1. Introduction

The Trojan asteroids are a collection of hundreds of thousands of objects located in the Sun-Jupiter's  $L_4$  and  $L_5$  points. The little information available about these objects' characteristics lead to the existence of multiple models for their formation and origin. In order to fully understand the mechanisms that originated these asteroids, a mission to them is required. Such mission could cast light into the formation and evolution of the Solar System and help answering questions about the formation processes that took place in the Kuiper belt. There is also a possibility that these asteroids harbor life, thus increasing their scientific value. [1, 2, 3]

The present paper deals with the trajectory design for a mission to the Trojan  $L_4$  cluster, due to its larger number of objects and variety asteroid types, relatively to  $L_5$ . [3]

Although a mission to these objects has never occurred, it is still possible to establish parallels with missions to other low-gravity bodies, like NASA's NEAR-Shoemaker [4] and Dawn [5] or ESA's Rosetta [6]. All of these spacecraft have in common the use of multiple gravity assist trajectories during the interplanetary travel to their targets.

By direct comparison, one can deduce that the same strategy should be applied to this paper's mission, as it can significantly reduce propellant costs. Additionally, Dawn proves that it is possible to operate a spacecraft safely inside of an asteroid cloud (i.e. main asteroid belt), while visiting one or more targets [5]. This means that it is possible to observe a variety of Trojan asteroids without any significant collisional risks to the spacecraft.

Through comparison with the three previously mentioned missions (i.e. NEAR-Shoemaker, Dawn and Rosetta), and the trends in today's space industry, a decision was made to utilize high thrust (or chemical) propulsion systems for this paper's mission. Main reasons for this are the more common use of this type of technology (relatively to low propulsion technologies), and the reduced travel times that they can achieve. With both these characteristics, the mission duration is expected to be close to Rosetta's (i.e. 12.5 years [6]), which was a scientifically complex mission: 21 payloads, distributed between an orbiter and lander. Furthermore, low mission durations lead to increased survivability and reduced operation costs.

As such, this paper's trajectory design will only

Phase	Asteroid rendezvous	Asteroid flyby tour
Interplanetary	Minimize total $\Delta V$	Minimize total $\Delta V$ Minimize $V_{rel}$
Science	Inside swarm	Minimize maneuvering $\Delta V$ Maximize number of asteroids seen
	Outside swarm	Minimize return DSM's $\Delta V$

Table 1: Objectives for the interplanetary and science phases of the two considered missions: single asteroid rendezvous and flyby tour.

consider high thrust maneuvers, similarly to what has been performed by Canalias et al. [7] in an analogous study. By utilizing Rosetta as reference, it is possible to establish a maximum allowed propellant-to-wet mass ratio of 0.56 [6], which is equivalent to a maximum on-board  $\Delta V$  of 3.5 km/s, if a high thrust system with a superior specific impulse ( $I_{sp}$ ) of 330 seconds is used [8], and a safety margin of 18% is taken into account on the fuel ratio. This constraint thus avoids the definition of a launcher, or of a maximum dry mass for the spacecraft, keeping the design of this paper flexible and focused on the mission's trajectories.

The chosen propulsion technology leads to only two mission types: **single rendezvous** and **flyby tour**. The first one consists of performing a rendezvous with a single asteroid. In the latter, introduced by Canalias et al. [7], the spacecraft would observe multiple asteroids by sequentially altering its trajectory and passing by various targets.

Both designs have different observational strategies, thus representing two optimization problems. Due to the amount of Trojan asteroids in  $L_4$  with known ephemeris (4087 [9]), and the number of available planets for gravity assists, the two mission designs must be divided into phases, in order for them to be practically solvable within this work's time limit. As such, each mission will be divided into an **interplanetary phase** (multiple gravity assist trajectories to the Trojan asteroids) and a **science phase** (asteroid-to-asteroid trajectories), similarly to Canalias' approach [7].

For the single asteroid rendezvous mission, the spacecraft travels to a Trojan object, inserting itself in its orbit. Therefore, there are no maneuvers in the science phase. Consequently, the interplanetary phase's goal is going to be the minimization of the total mission's  $\Delta V$ , including Earth's excess velocity, as this will help minimize the launcher's effort during the hyperbolic injection, and maximize the launch mass.

Regarding the flyby tour mission, due to the sectioning of the problem, the interplanetary phase will target the  $L_4$ , following Canalias' methodology [7]. The goal of this phase will be the minimization of

the total interplanetary  $\Delta V$ , and of the final relative velocity to  $L_4$  ( $V_{rel}$ ). The latter assures that the spacecraft is traveling slower at arrival, relatively to the swarm, which in turn results in longer observation times. Finally, in the science phase, the optimization goals are the minimization of the total in-swarm maneuvering  $\Delta V$  and the maximization of the observed asteroids. If there is a possibility to apply a deep space maneuver (DSM) after the first flyby tour, and return to the swarm for a second one, that maneuver's  $\Delta V$  will be minimized. The two phases' solutions will then be joined together by simply altering the last interplanetary leg's  $\Delta V$ , thus following the approach presented by Canalias et al. [7].

Both missions' objectives are summarized in Table 1, for each of their phases.

## 2. Spacecraft trajectory

Since the mission was divided into two phases — interplanetary and science — it is possible to describe their trajectories as separate design problems. Given the large search space for multiple gravity assist interplanetary trajectories, the common approach found in the literature is to utilize the MGA and MGA-1DSM formulations [10, 11]. These models parameterize the whole trajectory with a decision vector  $\mathbf{p}$ , which is translated into the cost function's value through the use of patch conics [12].

Inside the Trojan asteroid cloud, Jupiter's attraction (i.e. gravitational acceleration) is less than 1% of the local solar influence, which is not considered to be significant by this paper's author. Therefore, two-body approximations will continue to be adopted in the science phase, with the Sun as the central body. Due to the lack of information regarding the Trojan asteroids' mass and radii, patch conics are going to be used in the science phase as well.

In this section, both phases' trajectory models will be formally introduced, together with any equations that differ from their literature counterparts.

## 2.1. Interplanetary phase

As mentioned previously, MGA and MGA-1DSM will be utilized in the interplanetary phase. The former utilizes powered gravity assists and no DSM's, while the latter uses the opposite.

### MGA

The generic MGA problem can be formally described as:

$$\begin{aligned} & \text{Minimize} && J(\mathbf{p}) \\ & \text{w.r.t.} && \mathbf{p}, \\ & \text{subject to} && r_p(t_i) \geq \tilde{r}_p^i, \\ & \text{with} && \mathbf{p} = [t_0, T_1, \dots, T_N], \end{aligned} \quad (1)$$

where  $J$  is the cost function and  $\mathbf{p}$  is the decision vector [10]. The notation used describes epochs as  $t$ , leg durations as  $T$ , gravity assist's pericenter radii as  $r_p$  and safe radii as  $\tilde{r}_p$ .

Additionally,  $N$  is the number of planets in the sequence (excluding the starting one), and  $i$  symbolizes the  $i^{\text{th}}$  gravity assist. Therefore,  $t_i$  refers to the epoch at which the  $i^{\text{th}}$  gravity assist occurs. The leg durations allow for the determination of the heliocentric planet-to-planet (or target-to-target) trajectories with a Lambert solver. This work utilizes Izzo's algorithm [11] for computing Lambert solutions due to its faster computation time [13]. The resultant velocities of the Lambert trajectories define the incoming and departing relative velocities ( $\vec{v}_{in}$  and  $\vec{v}_{out}$ ) to each of the gravity assist's planets. With those, the pericenter radius, where the  $\Delta V$  is applied, is computed through the iterative method described in [11].

However, in case that  $r_p$  violates the condition in Equation 1, the implementations found in the literature use penalty factors in the calculation of the  $\Delta V$ . In this paper, those arithmetic penalty factors are substituted by an additional corrective maneuver, either at the point of encounter, or departure, of the gravity assist's planet. This increases the theoretical accuracy of the model.

If performed at the point of encounter, the corrective maneuver  $\Delta V_\alpha$ , at planet  $i$ , is given by:

$$\begin{aligned} \Delta V_\alpha &= \left| \|\vec{v}_{in}\| - v_{in}^{new} \right|, \\ \text{where} \quad v_{in}^{new} &= \sqrt{\frac{\mu_i}{a_{in}^{new}}}, \\ a_{in}^{new} &= \frac{\sin f(\alpha)}{1 - \sin f(\alpha)} \tilde{r}_p^i, \\ f(\alpha) &= \alpha - \arcsin \frac{a_{out}}{a_{out} + \tilde{r}_p^i}, \\ \text{with} \quad \alpha &= \arccos \frac{\vec{v}_{in} \cdot \vec{v}_{out}}{\|\vec{v}_{in}\| \|\vec{v}_{out}\|}, \\ \text{and} \quad a_{out} &= \frac{\mu_i}{\vec{v}_{out} \cdot \vec{v}_{out}}. \end{aligned} \quad (2)$$

In case this correction is done at the departure point, the value is given by:

$$\begin{aligned} \Delta V_\alpha &= 2 \|\vec{v}_{out}\| \sin \left( \frac{\Delta \alpha}{2} \right), \\ \text{where} \quad \Delta \alpha &= \alpha - \alpha_{max}, \\ \alpha_{max} &= \arcsin \frac{a_{in}}{a_{in} + \tilde{r}_p^i} + \\ &+ \arcsin \frac{a_{out}}{a_{out} + \tilde{r}_p^i}, \\ \text{with} \quad a_{in} &= \frac{\mu_i}{\vec{v}_{in} \cdot \vec{v}_{in}}. \end{aligned} \quad (3)$$

### MGA-1DSM

The generic MGA-1DSM problem can be formally described as:

$$\begin{aligned} & \text{Minimize} && J(\mathbf{p}) \\ & \text{w.r.t.} && \mathbf{p}, \\ & \text{with} && \mathbf{p} = [t_0, V_\infty, u, v, \\ & && T_1, \dots, T_N, \eta_1, \dots, \eta_N, \\ & && r_p^1, \dots, r_p^{N-1}, \beta_1, \dots, \beta_{N-1}], \end{aligned} \quad (4)$$

following the same notation described for Equation 1. Additionally,  $V_\infty$  represents the excess velocity modulus on Earth, with its vector's direction being described through Conway's equations [10], using variables  $u$  and  $v$ . Finally,  $\beta$  is the gravity assist's plane's orientation (in radians). All of the equations utilized to convert the decision vector into the cost function's value were the same as Conway's model's [10], so they will be spared from this paper.

## 2.2. Science phase

For the science phase, due to the low influence of Jupiter on the Trojan asteroids, relative to the Sun's, a two-body approximation will continue to be adopted, with the star as its central body. As mentioned previously, there is insufficient information regarding the Trojan asteroids' masses and radii, so patch conics trajectories will be investigated, approximating the objects as infinitesimal points, with no gravity.

In the applications of the literature, namely Canalias et al. [7] and Stuart et al. [3], Jupiter's influence was also taken into consideration. Therefore, the trajectory models utilized in this paper must differ from the ones presented in previous similar studies.

Looking at Canalias' model [7] in particular, since it was the only one found dealing with asteroid flyby tours, it is possible to see that the use of a three body approximation lead to the incorrect optimization of the tour's  $\Delta V$ . This was due to the complexity of the equations, which forced the model to optimize the tour's individual legs sequentially, in

order to make the computational effort reasonable. For example, in a sequence of asteroids A-B-C, this method would optimize the leg A-B, and from that solution it would search for the subsequent optimum B-C trajectory, which is theoretically incorrect, since all legs are dependent on the previous ones.

As such, a model was defined, inspired by the MGA formulation presented in Equation 1. For a particular asteroid tour sequence, this model computes the asteroid-to-asteroid trajectories using Lambert solvers. The impulsive maneuvers involved are computed by patching those trajectories at the points where the spacecraft encounters each individual target asteroid. In other words, this paper’s model adapts the MGA formulation, by substituting the powered gravity assist part (i.e. the calculations inside each target’s sphere of influence) with a simple heliocentric DSM.

This model’s generic form can be formally described as

$$\begin{aligned} &\text{Minimize} && J(\mathbf{p}) \\ &\text{w.r.t.} && \mathbf{p}, \\ &\text{with} && \\ &&& \mathbf{p} = [T_1, \dots, T_N], \end{aligned} \quad (5)$$

where the notation is the same as for Equation 1. Here,  $T$  represents the leg durations, but between asteroids. The departing epoch  $t_0$  is not included in the decision vector since its value is fully determined by the interplanetary phase’s solution.

The use of a global formulation, with a decision vector that fully determines the cost function, allows for the correct optimization of the tour’s total  $\Delta V$ . This is a major improvement relatively to Canalias’ model [7] and is expected to lead to better results, since global optimums can be more efficiently searched for.

### 3. Trajectory optimization

With the trajectory models defined in Section 2, the next logical step is to determine which optimization algorithms to utilize for the mission design. Logically, due to the stratification of the problem (i.e. interplanetary and science phases) and the different models implemented for each phase, multiple optimization algorithms can be applied for different sections.

Regarding the interplanetary phase, global optimization strategies are common to be implemented for MGA and MGA-1DSM trajectories [7, 10, 11, 13], due to the complex solution space of multiple gravity assist problems. The most common algorithms used are Differential Evolution (DE), Particle Swarm Optimization (PSO) and Artificial Bee

Colony (ABC). Due to the proven superiority of these algorithms in the mentioned literature, they will also be used in this paper.

All of the mentioned global optimization algorithms - and many more - are present in ESA’s PyGMO [14] toolbox for the Python language. Because of this toolbox’s extensive resources and algorithms, in global and local optimization problems, with one or multi-objectives, it will be used in this paper.

Due to the novelty of the science phase’s trajectory model, described in Equation 5, no direct conclusions can be drawn from the literature. However, since the model implemented, and its formal description, is a direct adaptation of the common MGA problem, it is possible to infer that global optimization techniques may be more efficient for this case.

In this section, the suitability of the already mentioned optimization algorithms will be discussed, both for the interplanetary and science phases. Additionally, tuning of each algorithm’s settings will be presented where it is seen fit.

#### 3.1. Interplanetary phase

In the interplanetary phase there are two types of trajectories: MGA and MGA-1DSM. Due to the differences in each model’s equations and impulsive maneuvers, different optimization algorithms might be needed. In this subsection, MGA will be firstly discussed, followed by MGA-1DSM.

#### MGA

For the MGA formulation there are two validation problems provided by GTOP [11]: Cassini 1 and GTOP 1. The only survey of optimization algorithms for MGA is found in [10], therefore no cross-referencing can be performed, in order to figure out which alternatives are consistently better. As such, a separate survey will be done in this paper, using the classic DE, PSO and ABC. Additionally, jDE [15] and mDE [16], which are self-adaptive variants of DE implemented in PyGMO, will be analyzed as well.

The initial survey was made with 100 different populations, which were evaluated 80,000 times in the case of Cassini 1, and 120,000 in the case of GTOP 1. These values were identical to what was performed by Conway [10], and so were the settings of the individual algorithms. In the case of jDE and mDE, the settings used were the default ones of PyGMO [14].

After the established number of function evaluations, the results obtained were the ones in Table 2. It can be immediately seen that jDE is able to achieve high accuracy results in both problems, which have significantly different solution spaces, due to the differing cost functions and optimization

Problem	Result	DE	jDE	mDE	PSO	ABC
<b>Cassini 1</b>						
	km / s					
Solution	4.9307					
	Mean	8.1993	9.3134	12.4063	12.8089	7.5247
	Min	5.3034	<b>4.9309</b>	<b>4.9307</b>	5.2547	5.7157
<b>GTOC 1</b>						
	kg km <sup>2</sup> / s <sup>2</sup>					
Solution	-1,581,950					
	Mean	-1,157,156	-1,170,525	-706,150	-610,642	-594,622
	Min	<b>-1,576,136</b>	<b>-1,581,928</b>	-1,387,410	-1,210,840	-997,893

Table 2: Results after 100 runs of the selected algorithms for both MGA validation problems, and comparison to the global minimum.

goals of Cassini 1 and GTOC 1. Furthermore, given that jDE also resulted in accurate mean values for the best individuals of the 100 populations in both problems, it is clear that this algorithm outperforms the rest in MGA formulations.

Given that jDE was not found to be applied in the literature for MGA optimization problems, there are no studies on the impact of its settings on the efficiency of the algorithm. Consequently, tuning of those settings must be investigated in this paper, as to minimize the computational effort required for the work.

PyGMO’s jDE implementation has two settings: the algorithmic variant (values of 1-18) and the adaptive scheme (1 or 2). The first one describes how the mutations in DE are computed, and the second one defines how DE’s parameters (weighting factor -  $F$  - and cross-over ratio -  $CR$ ) mutate throughout the computations.

As a reference, Cassini 1 will be used, as its cost function consists of a trajectory’s  $\Delta V$ , which is similar to what is going to be used in this paper’s interplanetary phase (see Table 1). The quantity used to evaluate the performance of each setting is  $n_{95\%}$ , which represents the number of function evaluations required to have 95% that the true solution has been obtained, with a maximum error of 50 m/s. This is similar to the strategy presented by Musegaas [13].

Following the computation scheme introduced in [13] as well, 100 populations were evaluated until a maximum of 80,000 function evaluations had been reached, or the best individual achieved the known global optimum. Of all the settings evaluated, the one that achieved the least average  $n_{95\%}$  used the **second algorithmic variant** and the **first adaptive scheme**. The mean  $n_{95\%}$  of that algorithm was close to  $2 \times 10^6$  function evaluations. These thus represent the optimum settings of the algorithm.

Applying a similar tuning process to the population size resulted in an optimum value of 20 indi-

viduals, achieving an average  $n_{95\%}$  of  $2 \times 10^6$ , and a minimum  $n_{95\%}$  of  $9 \times 10^5$ . Continuing to follow the process described by Musegaas [13], it is possible to relate the optimum population size ( $NP_{opt}$ ) with the number of variables in a problem ( $n_{var}$ ) linearly. With Cassini 1 having 6 variables,  $NP_{opt}$  results in

$$NP_{opt} = \frac{10}{3} n_{var}. \quad (6)$$

### MGA-1DSM

In the case of MGA-1DSM, there are multiple surveys available, most notably from Conway [10] and Musegaas [13], thus cross-referencing is possible. Both studies reached the conclusion that DE outperforms all other possible options for the optimizer.

In Musegaas’ M. Sc. thesis [13], an extensive study on the impact of DE’s settings in the minimum and average  $n_{95\%}$  values is presented. Therefore, and having in mind that this work’s goal is not focused on the optimization of optimizers’ settings, the results of that thesis will be utilized. These are summarized in Table 3.

These settings are able to achieve average  $n_{95\%}$  values of  $5 \times 10^6$ .

$F$	$CR$	Algorithmic variant	Population size
0.7	0.9	1 (best/1/exp)	$NP_{opt} = 4.5n_{var}$

Table 3: Best settings and population sizes for the DE algorithm applied to a MGA-1DSM formulation. [13]

### 3.2. Science phase

In the science phase, there is only one model, which was derived from MGA. Since its use is intended for asteroid flyby tours, and there are no similar studies in the literature, with comparable models, there are

no validation problems available.

However, since the developed formulation was adapted from the MGA model previously implemented, it is possible to draw comparisons from there. It is clear that the asteroid flyby tour is a simpler implementation than MGA, since the only difference is that the calculations inside each target’s sphere of influence were diluted to a single vector subtraction equation.

With that in mind, the solution spaces of the asteroid flyby tour are expected to be simpler. In other words, less local solutions should be present in each trajectory, since less maneuvering scenarios are allowed when only the heliocentric vectors are used.

Therefore, conservatively speaking, the same optimum optimizer for MGA (jDE) should continue to outperform all others in the asteroid flyby tour model. Extrapolating on that logical conclusion, the same optimum settings and population sizes should continue to yield faster computation times, since the solution spaces got their complexity reduced, relatively to MGA.

As such, jDE will continue to be used for the asteroid flyby tour, under the same optimum settings introduced in Section 3.1

## 4. Asteroid rendezvous mission

### 4.1. Input

Since the trajectory’s goal is to end in a particular Trojan asteroid, the multiple gravity assist sequences analyzed only considered planets from Mercury to Jupiter. Therefore, the planetary constants needed to perform the optimization of MGA or MGA-1DSM trajectories were those five planets’ gravitational parameters, radius and safe flyby radius. Additionally, the gravitational parameter of the Sun was required as well, since every interplanetary leg has the Sun as its focus. All of these constants’ values were obtained from PyKEP’s database [17].

In terms of ephemeris data, two different databases had to be used: for trajectories with 2 or less gravity assists SPICE [18] was utilized, with the remaining sequences being optimized under JPL-Low-Precision [19]. This change in database had to be performed due to the exponential increase in computational time with the number of gravity assists in a sequence. With these databases, the optimization time of a certain sequence’s population is always equal to, or under one hour.

Furthermore, for SPICE’s ephemeris, interpolation had to be implemented, since PyGMO could not load the kernels during the optimization. The interpolation step used was 0.1 days, thus achieving maximum positional errors of 369.3 km (occurring for Mercury). This maximum error is 37% of what is experienced by JPL-Low-Precision, for the same

planet.

Grav. assists	$\leq 2$	$> 2$
$t_0$ [mjd2000]	[7305, 10958]	[7305, 10958]
$V_\infty$ [km/s]	[0.1, 2.5]	[0.1, 2.5]
$u, v$	[0, 1]	[0, 1]
$T$ [days]	[30, 3000]	[30, 1826]
$\eta$	[0.01, 0.99]	[0.01, 0.99]
$\beta$ [rad]	$[-\pi, \pi]$	$[-\pi, \pi]$
$r_p$		
Rocky planets	$[\tilde{r}_p, 6\tilde{R}]$	$[\tilde{r}_p, 6\tilde{R}]$
Jupiter	$[\tilde{r}_p, 291\tilde{R}]$	$[\tilde{r}_p, 291\tilde{R}]$

Table 4: Boundary values introduced to the interplanetary phase’s optimization algorithm, in order to define the search space.

Finally, boundary values had to be defined for all variables in the decision vectors of MGA and MGA-1DSM. These were derived from GTOp’s problems [11], with a mission launch between 2020 and 2030, ending before 2050 (end of ephemeris range). These can be found completely defined in Table 4. The pericenter radius boundary was expressed as a function of the gravity assist’s planet’s radius  $\tilde{R}$ .

### 4.2. Results and discussion

For this type of mission, the optimization’s goal is to minimize the total  $\Delta V$ . This includes the powered gravity assist/DSM’s  $\Delta V$  (depending on if it’s an MGA or MGA-1DSM trajectory), the arrival impulse to the Trojan asteroid, and Earth’s excess velocity.

The chosen Trojan asteroid target is 624 Hektor, since it was presented as the most interesting scientific target by Stuart et al. [3].

In total, 101 sequences were analyzed, with zero to 3 gravity assists, for MGA and MGA-1DSM trajectories. The top trajectories are shown in Table 5. Each sequence’s name is composed by the first letter of each planet’s designation, with the exception of *Mer*, which corresponds to Mercury, and *H* which designates 624 Hektor. For example, an EMerVH sequence refers to a trajectory starting on Earth, passing through Mercury, Venus and finally arriving to 624 Hektor.

Table 5 shows detailed information regarding the top two sequences with a first flyby on Earth, and for the best four sequences without that gravity assist. Although this choice of top results seems odd, it is related to the fact that, when there is a first gravity assist on Earth, the initial Earth’s excess velocity is close to zero. With excess velocities that low, most of the  $\Delta V$  of the trajectory will have to be performed by the spacecraft, thus increasing its on-board fuel storage.

Sol.	Sequence	Departure date [UTC]	Duration [years]	$\Delta V$ [km/s]		
				Excess	GA's	Arrival
1	E-E-M-J-H	29/08/2028	10.0	0.0001	1.0754	3.3537
2	E-E-V-M-H	21/09/2026	5.8	0.0002	0.8476	4.3041
3	E-V-E-J-H	26/10/2029	9.3	2.8234	0.4553	3.2200
<b>4</b>	<b>E-M-J-H</b>	<b>18/01/2025</b>	<b>13.4</b>	<b>4.0388</b>	<b>1.7307</b>	<b>0.7365</b>
5	E-M-E-J-H	10/03/2029	9.9	3.4225	0.2553	3.2514
6	E-M-V-J-H	08/02/2029	10.0	3.2045	0.6989	3.2278

Table 5: Top solutions for the single asteroid rendezvous mission. All of the presented trajectories are of the MGA type. The chosen solution for the design is highlighted in bold font.

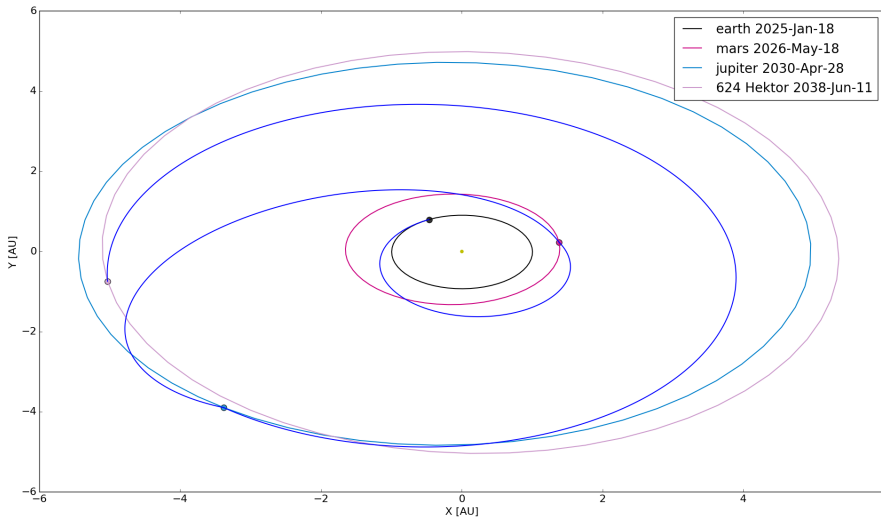


Figure 1: Final designed orbit for a rendezvous with 624 Hektor, departing from Earth on 10/03/2029. All ephemeris are presented in an ecliptic J2000 frame.

Taking into account the on-board  $\Delta V$  limit of 3.5 km/s, it is clear that solution 4 is the only feasible option. As such, it is chosen as the final designed trajectory. The path to 624 Hektor is shown in Figure 1.

## 5. Asteroid flyby tour mission

### 5.1. Input

For the interplanetary phase, the ephemeris data, boundary values and planetary constants used were the same ones listed in Section 4.1, since the trajectory models and optimization algorithms are identical.

Regarding the science phase, the asteroids' ephemeris were obtained from IAU's database [9] from June 20, 2016. In terms of boundary values, the asteroid-to-asteroid travel time was set to vary between 1 day and 2 years (730.5 days), as this encompassed all of the solutions presented by Canalias et al. [7].

### 5.2. Pruning

Due to the large number of targetable asteroids (4087 to be more precise [9]), pruning criteria had to be defined in order to restrict the search space, and respect the limited time available for this work. If all tours with five asteroids (maximum number of asteroids observed in Canalias et al. [7]) were analyzed in this work, then  $10^{18}$  would have to be investigated.

The first criteria chosen establishes that no tours with repeating asteroids in a sequence should be investigated, as those are less rich scientifically.

For the second and final criteria, a pruning process similar to the one of Canalias [7] was implemented. In order to provide a simple description, let us consider that there are a total of three targetable asteroids: A, B and C. First, the optimization software should determine every minimum  $\Delta V$  tour with sequences of two asteroids (i.e. A-B, A-C, B-C and vice-versa). With that information, the software identifies which sequences violate a certain

Sol.	Sequence	Departure date [UTC]	Duration [years]	$\Delta V$ [km/s]		$V_{rel}$ [km/s]
				Excess	GA's	
1	E-Mer-L	29/10/2023	2.7	9.6309	$\sim 10^{-8}$	4.1969
2	E-M-Mer-E-L	03/06/2020	10.2	7.4471	$\sim 10^{-8}$	4.3429
3	E-M-J-E-L	06/04/2027	8.7	4.2570	0.0022	4.6974
<b>4</b>	<b>E-V-Mer-V-L</b>	<b>01/04/2020</b>	<b>4.9</b>	<b>3.0318</b>	$\sim 10^{-10}$	<b>5.0961</b>
5	E-E-Mer-V-L	28/08/2024	4.7	0.0002	2.3139	5.5173
6	E-E-V-V-L	28/12/2021	5.8	0.0002	1.4392	6.1835
7	E-E-M-E-L	22/02/2022	5.1	0.0001	0.9098	6.6738

Table 6: Pareto front solutions of the interplanetary optimization of the asteroid flyby tour mission. All of the presented trajectories are of the MGA type. The chosen solution for the design is highlighted in bold font.

maximum allowed value on total  $\Delta V$  ( $\Delta V_{max}$ ) (interplanetary maneuvering included), and add one asteroid to the ones who do not. For example, consider that  $\Delta V_{A-B}$  and  $\Delta V_{A-C}$  resulted in 1 and 10 km/s, respectively, and that  $\Delta V_{max}$  was set to 5 km/s. In that particular case, the optimization software would then investigate a tour of A-B-C, but not a tour of A-C-B, since the latter started with a trajectory from A to C that already violated the limit defined. For this work, the described pruning logic is extended to 4087 Trojan asteroids, and  $N$  asteroid sequences. With it, the number of asteroid sequences investigated is severely reduced.

One of the main advantages of this work is the possibility of directly comparing every result with the ones obtained by Canalias et al. [7]. As such, different  $\Delta V_{max}$  values were set, depending on the number of asteroids  $N$  observed, based on the best solutions presented by Canalias et al. [7]. Their values are shown in Table 7. To clarify, the values presented in the table refer to the limit that any  $N$  asteroid sequence has to respect, in order for it to be propagated to  $N + 1$ . Naturally, the limit set for one asteroid sequences is applicable to the sum of the on-board  $\Delta V$ 's involved in the interplanetary trajectory, including the adjustment needed to target the initial asteroid.

$N$	1	2	3	4	$\geq 5$
$\Delta V_{max}$ [km/s]	0.5	0.7	1.2	1.5	3.5

Table 7: Maximum  $\Delta V$  values (for the whole mission) allowed for an  $N$  asteroid sequence to be propagated into  $N + 1$ . Values based on the top results of Canalias et al. [7].

### 5.3. Results and discussion

For the interplanetary phase, the cost function utilized was the sum of Earth's excess velocity, with the  $\Delta V$ 's required to arrive to the  $L_4$ . The planetary sequences analyzed were the same as from

Section 4, with MGA trajectories proving to yield better  $\Delta V$  results than MGA-1DSM.

The optimization results of the interplanetary trajectory were then studied as a Pareto Front, taking into account the total  $\Delta V$  and the relative velocity of arrival to the  $L_4$ ,  $V_{rel}$ . The Pareto front solutions, which are all of the MGA type, are shown in detail in Table 6. It should be noted that, in the sequences' names,  $L$  denotes the  $L_4$ .

Out of all the solutions presented, using the manuals for Soyuz [20] and Delta IV [21], and the high thrust propulsion system described in Section 1, it is possible to deduce that solution 4 is better, since it leads to higher arrival masses to  $L_4$ . As such, it was chosen as the design of this mission's interplanetary phase. This solution represents savings of 200–400 m/s relatively to Canalias' designed interplanetary trajectories [7].

With this solution's decision vector, the adjustments needed to target the first asteroid of every sequence were performed by correcting the last gravity assist's  $\Delta V$ . With that correction, the results of the science phase were obtained by optimizing the total maneuvering  $\Delta V$  associated with them (including the correction to the last interplanetary leg). More than  $10^9$  sequences were analyzed, of which approximately only 44,000 were within the pruning boundaries.

The solution that resulted in the observation of more Trojan asteroids managed to encounter six, which is one more than Canalias' top result [7], requiring 2.3903 km/s of total on-board  $\Delta V$ . Naturally, since the main goal of this optimization was to maximize the number of asteroids in the tour, this is the chosen design for the mission. This trajectory's characteristics are listed in Table 8.

A plot of the total trajectory of this design is also evidenced in Figure 2, in the ecliptic J2000 reference frame.

	Epoch [UTC]	$\Delta V$ [km/s]
<b>Interplanetary</b>		
Earth	01/04/2020	–
Venus	21/09/2020	$\sim 10^{-10}$
Mercury	27/11/2020	$\sim 10^{-10}$
Venus	11/07/2022	0.0300
<b>Science</b>		
2000QD225	16/02/2025	0.4175
2010UQ91	24/08/2025	0.5097
2008KT37	26/11/2025	0.4102
2012QV34	19/01/2026	0.4357
1997UL16	28/01/2026	0.5872
2002GO29	30/03/2026	–

Table 8: Detailed breakdown of encounter epochs and  $\Delta V$ 's associated with the best trajectory obtained for the asteroid flyby tour mission.

Besides the solution presented, 19 of the computed trajectories were superior to Canalias' top results [7], encountering 3 to 5 asteroids. The improvements in  $\Delta V$  were all less than 400 m/s, thus validating the processes used in the optimizations of this work, and the models developed for it.

Unfortunately, all computed tours, with  $\Delta V$ 's within pruning boundaries, lead to eccentric anomaly values larger than  $180^\circ$  at the point of encounter with the last asteroid in the sequence. This means that, after all computed feasible sequences,

the spacecraft is always exiting the swarm through its sun-lit side. Consequently, it is impossible to investigate return DSM's that would take the spacecraft back to the cloud to perform a second tour, as these would lead to unfeasible  $\Delta V$ 's. As such, that maneuver will not be analyzed in this work.

## 6. Conclusions

This thesis' goal was to design the trajectories for a mission to the Trojan asteroids. Two different observational strategies (i.e. single asteroid rendezvous and flyby tour) were defined in Section 1, by comparing literature studies with the high thrust propulsion system. These two strategies resulted in two different designs, with two very distinct trajectories.

For the single asteroid rendezvous mission, an interplanetary multiple gravity assist trajectory of the MGA type was obtained, with an EMJ path to asteroid 624 Hektor, and requiring 2.4672 km/s of on-board  $\Delta V$ .

Regarding the asteroid flyby tour, a final interplanetary path of EVMerV was obtained, with powered gravity assists, resulting in the final observation of 6 different asteroids, and consuming a total on-board  $\Delta V$  of 2.3903 km/s. This design represents an improvement relatively to Canalias et al. [7], since it leads to the observation of one extra Trojan asteroid. The remaining best trajectories, observing five or less asteroids, resulted in  $\Delta V$  savings of  $< 400$  m/s, when compared to Canalias' top results [7]. This validates the quality of the opti-

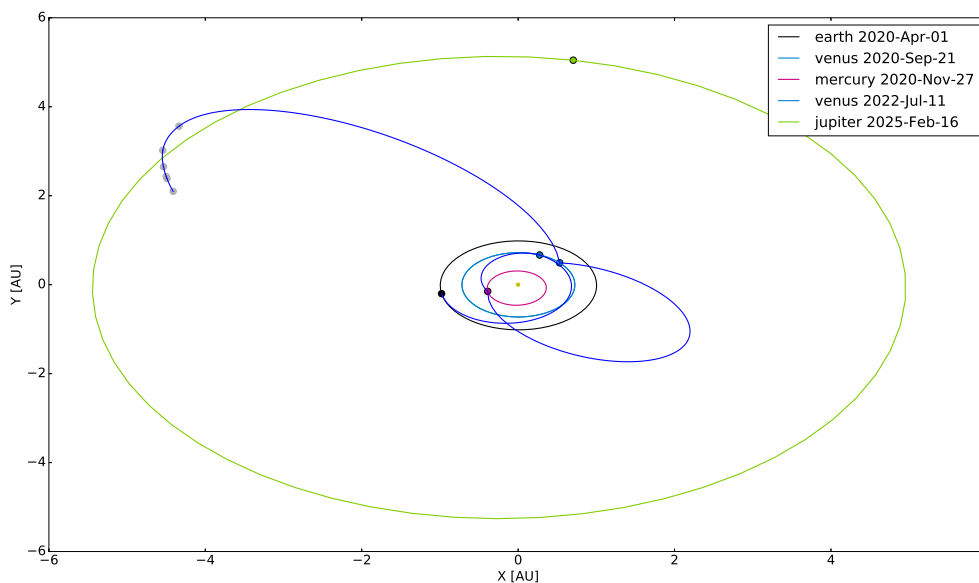


Figure 2: Final designed orbit for the asteroid flyby tour mission, departing from Earth on April 1, 2020 and encountering 6 asteroids. All ephemeris are presented in an ecliptic J2000 frame.

mization processes implemented and, more importantly, of the asteroid tour trajectory model, fully developed by this work's author. It is then proved that, by improving Canalias' trajectory model, expanding it into global optimization, better results can be obtained.

In conclusion, the feasible trajectories designed for both missions (i.e. single rendezvous with 624 Hektor and flyby tour), together with their improvements with respect to Canalias' results [7], are considered to be important achievements of this work. Considering that the top-level objective of this thesis was achieved, and that the solutions are feasible to be applied to real space missions, the work developed is regarded as a success.

## References

- [1] Gy. M. Szabo et al. "The properties of Jovian Trojan asteroids listed in SDSS Moving Object Catalogue 3". In: *Monthly Notices of the Royal Astronomical Society* 377.4 (June 2007).
- [2] Joshua P. Emery et al. "The complex history of Trojan asteroids". In: *Asteroids IV*. University of Arizona Press, 2015, pp. 203–220.
- [3] Jeffrey A. Stuart, Kathleen C. Howell, and Roby S. Wilson. "Design of end-to-end Trojan asteroid rendezvous tours incorporating scientific value". In: *Journal of Spacecraft and Rockets* 53.2 (Mar. 2016), pp. 278–288.
- [4] NASA. *NEAR-Shoemaker mission description*. <http://science.nasa.gov/missions/near/>. Retrieved in: 26-04-2016.
- [5] *Dawn mission description*. <http://dawn.jpl.nasa.gov/mission/>. Retrieved in: 26-04-2016.
- [6] ESA. *Rosetta mission description*. [http://www.esa.int/Our\\_Activities/Space\\_Science/Rosetta](http://www.esa.int/Our_Activities/Space_Science/Rosetta). Retrieved in: 11-10-2016.
- [7] Elisabet Canalias, Angffdfddla Mithra, and Dennis Carbonne. "End-to-end trajectory design for a chemical mission including multiple flybys of Jovian Trojan asteroids". In: *Advances in the Astronautical Sciences* 142 (2012), pp. 1195–1212.
- [8] James R. Wertz, David F. Everett, and Jeffrey J. Puschell. *Space Mission Engineering: The New SMAD*. Space Technology Library, 2011.
- [9] International Astronomical Union. *Ephemeris of Jupiter's Trojans*. <http://www.minorplanetcenter.net/iau/lists/JupiterTrojans.html>. Retrieved in: 15-08-2016. Apr. 2016.
- [10] Bruce A. Conway. *Spacecraft Trajectory Optimization*. Cambridge University Press, 2014.
- [11] ESA ACT - Informatics and Applied Mathematics. *Global trajectory optimization problems database*. <http://www.esa.int/gsp/ACT/inf/projects/gtop/gtop.html>. Retrieved on: 09-04-2016.
- [12] K. F. Wakker. *Astrodynamics-I lecture notes*. TU Delft, Mar. 2010.
- [13] Paul Musegaas. "Optimization of space trajectories including multiple gravity assists and deep space maneuvers". M. Sc. thesis report. Delft University of Technology, Dec. 2012.
- [14] *PyGMO* package. <http://esa.github.io/pygmo/index.html>. Retrieved in: 12-09-2016.
- [15] Janez Brest, Viljem Zumer, and Mirjam Sepesy Maucec. "Self-adaptive Differential Evolution algorithm in constrained real-parameter optimization". In: *2006 IEEE Congress on Evolutionary Computation* (July 2006), pp. 215–222.
- [16] Swagatam Islam, Subhrajit Ghosh, and Ponuthurai Suganthan. "An adaptive Differential Evolution algorithm with novel mutation and crossover strategies for global numerical computations". In: *IEEE Transactions on Systems, Man, and Cybernetics, Part B (Cybernetics)* 42.2 (Apr. 2012), pp. 482–500.
- [17] *PyKEP* package. <https://esa.github.io/pykep/>. Retrieved in: 12-09-2016.
- [18] *The SPICE Toolkit*. <https://naif.jpl.nasa.gov/naif/toolkit.html>. Retrieved in: 24-06-2016.
- [19] *JPL-Low-Precision*. [http://ssd.jpl.nasa.gov/?planet\\_pos](http://ssd.jpl.nasa.gov/?planet_pos). Retrieved in: 24-06-2016.
- [20] STARSEM - The Soyuz Company. *Soyuz User's Manual - Issue 3 - Revision 0*. Apr. 2001.
- [21] ULA - United Launch Alliance. *Delta IV - Payload Planners Guide*. Sept. 2007.